Journal of Solid State Chemistry 182 (2009) 1780–1785

Contents lists available at ScienceDirect

Journal of Solid State Chemistry

journal homepage: www.elsevier.com/locate/jssc

Direct crystallization of perovskite phase in PMN–PT thin films prepared by polyvinylpyrrolidone modified sol–gel processing and their properties

Z.H. Du [a,b,*], T.S. Zhang [c], M.M. Zhu [b], J. Ma [a,b]

[a] Temasek Laboratories, Nanyang Technological University (NTU), Singapore 637553, Singapore
[b] School of Materials Science and Engineering, NTU, Singapore 639798, Singapore
[c] Institute of Materials Research and Engineering (IMRE), Research Link, Singapore 117602, Singapore

ARTICLE INFO

Article history:
Received 1 August 2008
Received in revised form
14 April 2009
Accepted 19 April 2009
Available online 3 May 2009

Keywords:
PMN–PT thin films
PVP
Perovskite crystallization
Electrical
Optical properties

ABSTRACT

A modified sol–gel processing has been developed by using polyvinylpyrrolidone (PVP) as modifier and lead nitrate as lead source to synthesize $(1-x)Pb(Mg_{1/3},Nb_{2/3})O_3$–$xPbTiO_3$ (PMN–PT) thin films with $x = 0.23$–0.43. With PVP additions, perovskite phase could directly crystallize from amorphous films at the temperature as low as 430 °C via bypassing the metastable phase-pyrochlore and crystallinity was significantly enhanced. The PVP addictives have been optimized with molecular weight <630 K and the ratio of PVP monomer/PMN–PT at 0.25–1.0. XPS analysis indicates that the chemical states of the elements in the well-crystallized PMN–PT films are close to the literature data for the PMN–PT single crystals and the films possess highly desired electrical and optical properties.

1. Introduction

Initiated by Pechini in the 1960s [1], polymer species plays more and more important roles in sol–gel processing of various oxide films, especially at the beginning of this century. The polymers with carbonyl and/or ether groups can form complexes with metal ions and sterically entrap them in an entangled polymer network, resulting in homogenous and stable solutions. Furthermore, the combustion of polymers generates large amount of heat and increases the in situ temperature of gel particles. As a result, the formation of intermediate phases can be suppressed and single-phase materials can be obtained. For examples, polyethylenimine (PEI) have been used in synthesis of pure oxide films like $SrTiO_3$, $Ba_{1-x}Sr_xTiO_3$, and TiO_2 [2]. Polyethylene glycol (PEG), polyvinyl alcohol (PVA) and poly(vinyl acetate) (PVAc) have been used to prepare single-phase calcium aluminate ($CaAl_2O_4$), yttrium aluminate ($Y_3Al_5O_{12}$), and $Pb(Zr,Ti)O_3$ (PZT), respectively [3–5]. PEG is also found to be beneficial to prepare those ferroelectric oxides with less low thermally stable perovskite structure. $Pb(Zn_{1/3}Nb_{2/3})O_3$–$PbTiO_3$ (PZN–PT) and $(Pb(Zn_{0.6}Mg_{0.4})_{1/3}Nb_{2/3})O_3$–$PbTiO_3$ (PZMN–PT) thin films with pure perovskite structure have been obtained at the annealing temperature as low as 580 °C [6,7].

Polyvinylpyrrolidone (PVP), as a stress-relaxing agent, has been extensively applied to synthesize ceramic films, such as $BaTiO_3$, $BaBi_4Ti_4O_{15}$, PZT and PLZT with high critical thickness (one-coating thickness without cracking) of 0.4–1.2 μm [8–10]. PVPs were also used in preparation of ferroelectric nanofibers and nanometric particles [11,12]. However, it should be pointed out that the effect of PVPs on perovskite crystallization of various ferroelectric thin-film systems is received little attention in literatures. Our previous studies on PLZT films show that PVP promoted the formation of perovskite phase and reduced the onset crystallization temperature to around 450 °C with comparison of 540 °C for the non-PVP films [13]. It is therefore interesting to extend such studies to some other ferroelectric films (e.g. PMN–PT), in which the undesired pyrochlore phase is difficult to remove. Although PMN–PT films with pure perovskite structure have been obtained by some research groups, pyrochlore phase often dominated at low temperatures and can be completely removed only at annealing temperatures as high as ⩾700 °C [14–16]. As Pb will evaporate at high temperatures, the crystallized perovskite phase will decompose to pyrochlore phase again [17,18]. This, in turn, has resulted in reproducibility issues with the existing procedures.

PVPs exhibit some superior advantages in assisting the sol–gel synthesis of PMN–PT thin films. For examples: (1) PVPs could coordinate with metal ions by its carbonyl (C═O) or C–N groups

* Corresponding author at: Temasek Laboratories, 9th Storey, Research Techno-plaza, BorderXBlock, Nanyang Technological University (NTU), 50 Nanyang Drive, Singapore 639798, Singapore. Fax: +65 67900920.
E-mail addresses: duzehui@ntu.edu.sg (Z.H. Du), tszhang@ntu.edu.sg (T.S. Zhang), zhum0004@ntu.edu.sg (M.M. Zhu), asjma@ntu.edu.sg (J. Ma).

0022-4596/$ - see front matter © 2009 Elsevier Inc. All rights reserved.
doi:10.1016/j.jssc.2009.04.021

in every repeat unit [19,20] and meanwhile form hydrogen bonds to –OH, the common end groups of gel particles [21], probably leading to special ion distribution in sol–gel solutions which is beneficial for the desired phase formation and (2) the occurrence of large amount of heat as a result of combustion of PVPs instantly increases the in situ temperature of gel particles, especially when the strong oxidizer, i.e. lead nitrate is used as lead source to accelerate the combustion procedure. Hence low-temperature intermediate phases—pyrochlore can be circumvented and direct crystallization of perovskite phase from amorphous matrix can be realized.

In our previous work [22], PMN–PT films have been prepared by PVP modified sol–gel processing and PVPs were found to significantly promote the crystallization of perovskite phase. The films with PT% = 43 mol%, instead of the morphotropic phase boundary (MPB) composition (33 mol%), were chosen to investigate the crystallization kinetics of perovskite phase. The reason is that the perovskite crystallization in the PMN–PT films with lower PT content and prepared from non-PVP sols is less sensitive to the heating temperature and time, which induced some difficulties in studying the perovskite-crystallization kinetics. In this work, PMN–PT films with 43 mol% PT continued to be a model material to study the effect of PVP content and molecular weight on the crystallization behavior of perovskite phase. With the optimized PVP addition conditions, the crystallization of the PMN–PT films with 23–43 mol% PT has also been presented. The chemical states of the elements in the well-crystallized PMN–PT films were studied by high resolution XPS (X-ray photoelectron spectroscopy). Finally the electrical and optical properties of the films have been characterized.

2. Experimental

2.1. Preparation

For preparation of the thin films $(1-x)Pb(Mg_{1/3}Nb_{2/3})O_3$–$x$ $PbTiO_3$ ($x = 0.23$–0.43, 0.05 as interval), lead nitrate, magnesium acetate (vacuum dehydrated), niobium ethoxide, and titanium iso-propoxide were chosen as starting materials and 2-methoxyethanol (2-MOE) was used as a solvent. The polymer additives used include PVP10 (PVP with Mw = 10k, similar in the following), PVP40, PVP360, PVP630 and PVP1300, and the molar ratio of PVP monomer to PMN–PT was varied in 0–1.5. To compensate the Pb evaporation during post annealing, 15 mol% of Pb excess with respect to the stoichiometric amount was added. The precursor solutions leading to PbO, $Mg_{1/3}Nb_{2/3}O_3$ and TiO_2 were prepared, respectively, and then mixed together according to the flow chart shown in Fig. 1. PVPs were then added into the mixed solution and vigorously stirred for 12 h.

2.2. Characterization

Thermal decomposition behaviors of the PMN–PT (43% PT) dry gels with and without PVP360 modification were studied by DTA–TGA at a heating rate of 10 °C/min, in air atmosphere. The gel samples were obtained by drying the solutions at 100 °C for ~8 h and then thoroughly grinding. PMN–PT films were spin-coated on the substrates of PLT ($(Pb_{0.86},La_{0.14})TiO_3$)/ITO(indium tin oxide)/glass or PLT/1737 glass (Corning) from the as-prepared sol–gel solutions. The preparation procedure of the substrates can be found in our previous report [23]. The as-coated films were pyrolyzed at 430 °C for 10 min on a hot plate and then immediately transferred into an electric furnace to anneal at 430–650 °C for 30 min. Multi-layer samples with the thickness of ~0.8 μm were prepared by repeating 15 cycles of the coating and pyrolysis and then pre-annealed at 650 °C for 5 min every three coatings. The samples were finally annealed at 650 °C for 30 min for characterization of electrical and optical properties.

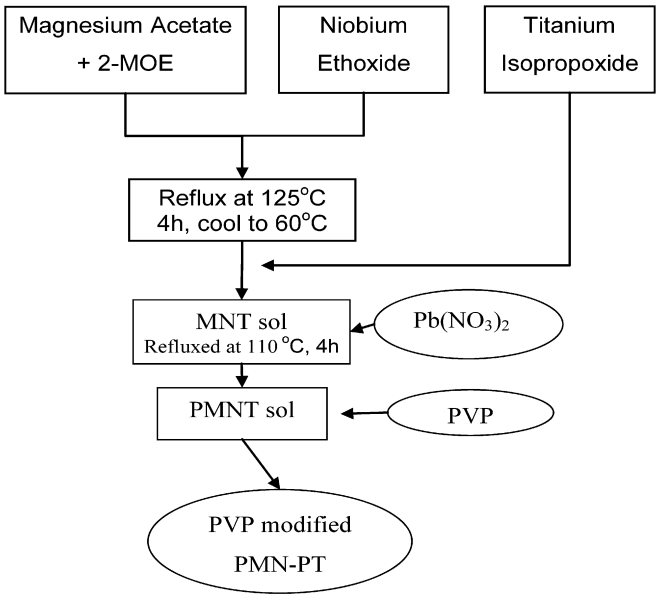

Fig. 1. Flow chart for the preparation of PMN–PT sol–gel solutions.

The crystallization of the PMN–PT films was studied by Rigaku ultima type X-ray diffractometer (XRD) with an incident angle of 1°. The morphologies of the films were examined using a field emission scanning electronic microscopy (FESEM, JSM-6340F, JEOL, Japan). The chemical states of the elements in the PMN–PT films annealed at 650 °C for 30 min were also studied by XPS spectrometer (PHI 04-500, Perkin–Elmer) using a Mg $K\alpha$(1253.6 eV) X-ray source operated at 15 kV, 20 mA emission conditions. The data were corrected by the reference of adventitious C1*s* Binding energy (B.E.) at 285.0 eV and analyzed by the software of CasaXPS (Version 2.3.12, Casa Software Ltd).

The electrical properties of the multi-layer samples (~0.8 μm thick) were studied by a standard Radiant RT6000HVS type ferroelectric tester and HP 4194A Impedance/Gain Phase Analyzer with 1 V ac voltage. The measurement area is 0.5 mm in diameter, coated with a layer of Pt (~100 nm thick) by sputtering. The optical properties of the films were measured by UV–Vis spectrometer (UV-2501PC, Shimazu) and Prism coupler (Metricon 2010) coupled with prism 200-P-2.

3. Results and discussion

3.1. Thermal analysis of the PMN–PT gels

Fig. 2 shows the TG–DTA curves of PMN–PT (43% PT) dry gels, together with that of pure lead nitrate. For the gel without adding PVP, two exothermic peaks can be identified at ~151 and ~311 °C. They are accompanied with a significant weight loss of ~17.1% at the temperature ⩽410 °C. The exothermic peaks and weight loss can be attributed to the decomposition of alkoxyl groups from the Mg, Nb and Ti precursors [24]. Moreover, two endothermic peaks were found at 434 and 452 °C, respectively, accompanying with a significant weight loss of 12.7%. These peaks can be ascribed to the decomposition of lead nitrate since similar endothermic peaks can also be found at ~452 °C in the TG–DTA curves of pure lead nitrate

and some intermediate phases like $Pb_2O(NO_3)_2$, $Pb_3O_2(NO_3)_2$ and/or $Pb_5O_4(NO_3)_2$ could be formed [25,26]. The intermediate phases from the decomposition of PMN–PT gels and pure lead nitrate should be different as another two endothermic peaks at 500 and 537 °C were found in the TG–DTA curves of pure lead nitrate, but not in that of PMN–PT gels. Further decomposition of the intermediate phases in the PMN–PT gels caused a broad exothermic peak and weight loss of 2.3% at 460–602 °C.

For the PMN–PT gels with PVP360 addition of 0.5 (PVP/PMN–PT), two exothermic peaks were located at ~190 and ~311 °C and can be attributed to the decomposition of Mg, Nb and Ti alkoxides. Another strong exothermic peak at ~456 °C was accompanied with a significant weight loss of ~14% at the temperature range of 350–500 °C. These can be ascribed to the strong combustion reactions between PVPs and $Pb(NO_3)_2$. When the PVP content was increased to 1.0, the exothermic peak at ~456 °C became extremely strong, indicating large amount of heat has been generated. This has been identified to be beneficial to perovskite formation, as will be demonstrated in the following.

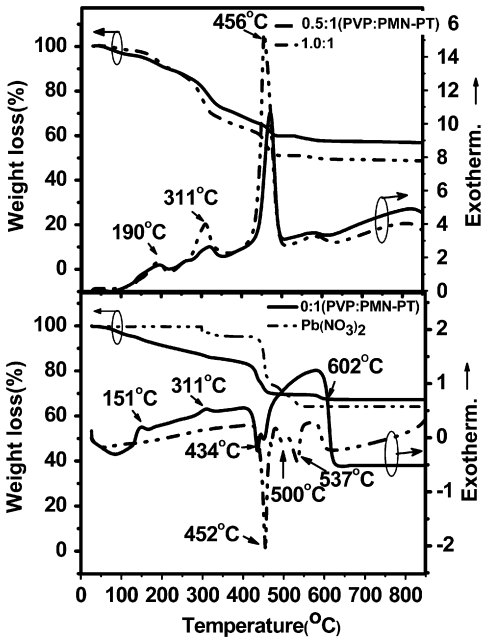

Fig. 2. TG–DTA curves of PMN–PT (43% PT) dry gels with different PVP360 additions.

3.2. Effect of PVP content on the crystallization of PMN–PT films

Fig. 3(a)–(f) presents the XRD patterns of one-coating 0.57PMN–0.43PT films prepared from the modified sol–gel solutions with different PVP360 contents and annealed at 430 °C for 30 min. A peak corresponding to pyrochlore phase was found in the films without PVP modification (Fig. 3(a)), while for the films with PVP additions, only perovskite phase can be detected and the crystallization degree of the perovskite phase increased with PVP content increasing (Fig. 3(b)–(f)). The onset temperature of perovskite formation for the PVP-modified films was therefore to be 430 °C or less, which is much lower than the literature values (i.e. 550–700 °C) [14–28]. Pyrochlore phase, the intermediate product during perovskite crystallization, was not detected in the films with PVP addition of 0.25–1.0 and annealed at 460–650 °C (Fig. 3(h)–(l) and (n)–(q)) except the films with PVP addition of 1.5 and heated at 650 °C (Fig. 3(r)). In the films without PVP addition, the peak intensities of perovskite and pyrochlore phase were concurrently increased after heating at 460 °C (Fig. 3(g)) and the pyrochlore phase was still present even after annealing at 650 °C (Fig. 3(m)). The XRD results clearly showed that the optimal content of PVPs was in the range of 0.25–1.0, with which the formation of pyrochlore was suppressed and the crystallization of perovskite phase was enhanced.

The morphology of the PMN–PT films with different PVP additions and annealed at 650 °C for 30 min was shown in Fig. 4. The films without PVP modification consisted of the particles ~50 nm in size and some much smaller particles (highlighted by circles in Fig. 4(a)). The fine particles possibly belonged to pyrochlore phase since it has a relatively low crystallinity as compared with the perovskite phase (Fig. 3(m)). The films with PVP addition of 0.25–1.0 (only perovskite phase) have very uniform grain-size distribution (Fig. 4(b) and (c)). Meanwhile, PVP content has been found to have a significant influence on the densification of the films. The optimal content was identified to be 0.5–1.0 (e.g. Fig. 4(c)) since the samples with both lower (Fig. 4(b)) and higher PVP contents (Fig. 4(d)) exhibited porous

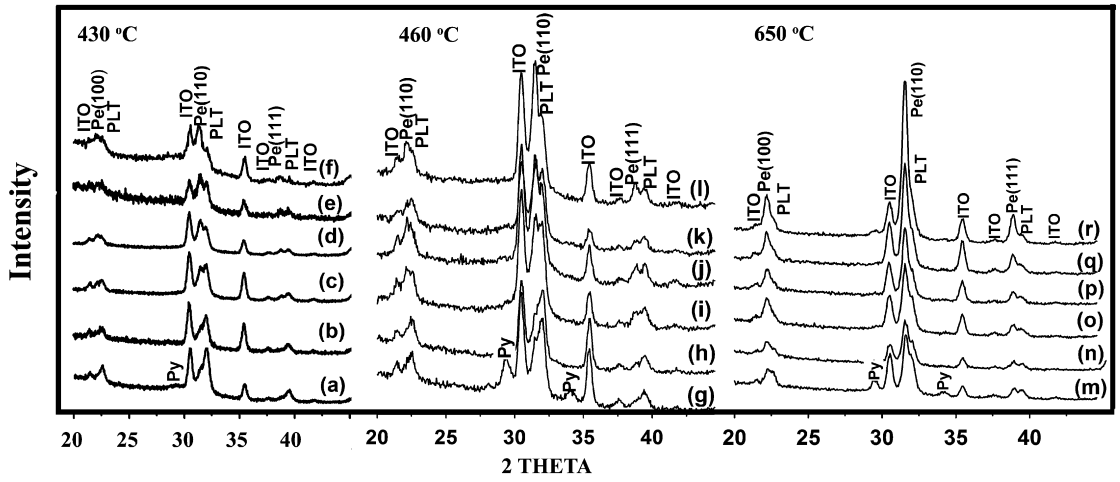

Fig. 3. XRD patterns of the one-coating 0.57PMN–0.43PT films on PLT/ITO/Glass substrates with different PVP360 monomer molar ratio to PMN–PT:(a), (g) and (m) 0, (b), (h) and (n) 0.25, (c), (i) and (o) 0.5, (d), (j) and (p) 0.75, (e), (k) and (q)1.0, (f), (l) and (r) 1.5. The films were heated at 430 °C (a)–(f), 460 °C (g)–(l) and 650 °C (m)–(r) for 30 min, respectively. Pe and Py stand for perovskite and pyrochlore phase, respectively.

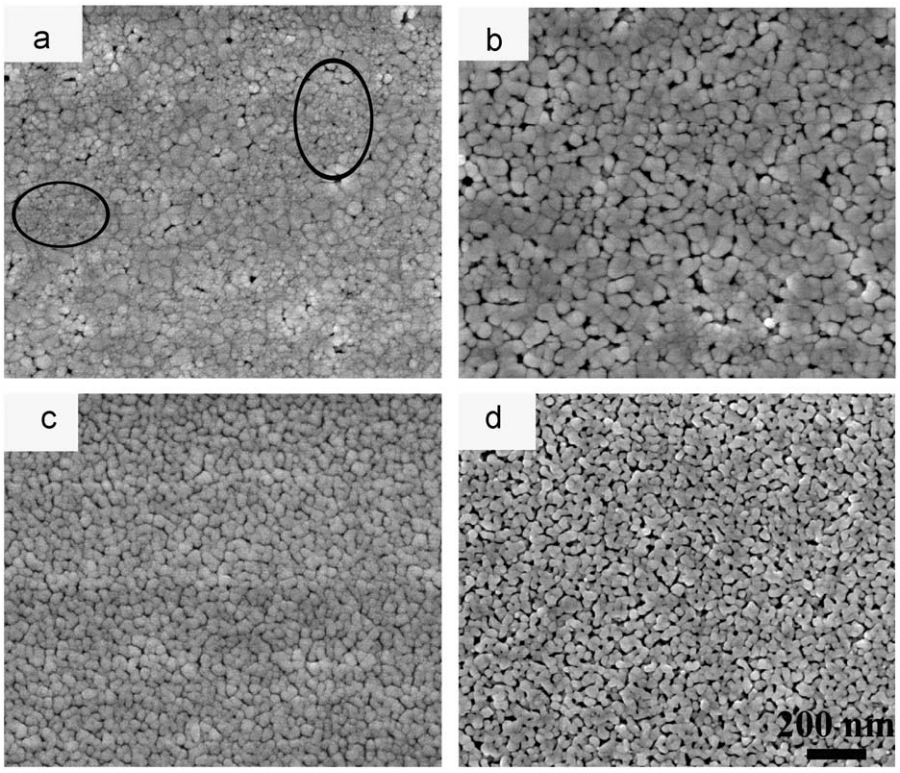

Fig. 4. FESEM images of the one-coating 0.57PMN–0.43PT films with PVP360 modification (a) 0, (b) 0.25, (c) 1.0, (d) 1.5 (molar ratio of PVP monomer to PMN–PT) and annealed at 650 °C for 30 min.

structures. The porous morphology with higher PVP content (Fig. 4(d)) can be attributed to the fact that the decomposition of excessive polymer in the films left lots of voids during crystallization. However, an explanation is unavailable at this stage regarding the porous structures of the films with lower PVP content (Fig. 4(b)).

3.3. *Effect of PVP molecular weight on the crystallization*

The effect of molecular weights (Mw: 10k–1300k) of PVPs on the crystallization behavior of the 0.57PMN–0.43PT films was also studied with the molar ratio of PVP monomer to PMN–PT fixed to be 1.0. When the films were heated at 460 °C for 30 min, perovskite phase was dominated in all the films studied and the peak intensity of perovskite increased with the increase of PVP molecular weight. Pyrochlore phase was detected only in the films modified by PVP with long molecular chains (e.g. PVP630 and PVP1300). After annealing at 650 °C for 30 min, however, only perovskite formed in all the films with good crystallinity. (The XRD patterns can be found in Figures S1 and S2 in "Supporting Information".) To avoid the formation of pyrochlore phase at low annealing temperatures, the optimal molecular weight of PVP should be < 630k. Furthermore, the densification of the films will be enhanced when the PVPs with smaller molecular weight were used.

3.4. *Crystallization of* $(1-x)$PMN$-x$PT *films around MPB*

$(1-x)$PMN–xPTs with compositions in the vicinity of MPB (i.e. $x = 0.23$–0.43) are always a research focus due to its disputable phase transition and promising electrical and optical properties. However, it is difficult to obtain high-quality samples since pyrochlore phase usually accompanies with lower PT contents. It is therefore interesting to investigate the effect of PVP addition on the phase formation of PMN–PT films with the compositions around MPB. Based on the optimized PVP addition conditions above, PVP40 was used to modify the sol–gel solutions with the molar ratio to PMN–PT equal to 1.0.

At the annealing temperature of 460 °C, only strong perovskite peaks were detected in all the PMN–PT films (the XRD patterns can be found in Figures S3 and S4 in the "Supporting Information"). When the annealing temperature was increased to 650 °C, similar XRD patterns were obtained for all the films except the sample with 23% PT that contained small amount of pyrochlore phase. This indicates that the PVP addictives play a crucial role in the formation of pure perovskite phase. If without PVP additions, it is difficult to obtain the pure-perovskite PMN–PT films even with a higher PT content (43%), as shown in Fig. 3(a), (g) and (m).

Perovskite phase most likely formed directly as a result of PVP addiction from the amorphous PMN–PT films, instead of following the well-recognized crystallization route: Amorphous → Pyrochlore phase → Perovskite phase. This can be attributed to the reduction of activation energy for perovskite crystallization and the in situ heat generated by the combustion of PVPs, according to our preliminary work [22]. More thorough mechanisms on the change of perovskite crystallization route could be found by further investigating the chemical reactions occurring in the PVP modified sol–gel solutions in the future. It is worth mentioning that the sol–gel processing by using both nitrate as lead precursor and PVP as energy releaser may be also helpful in preparing the other ferroelectric crystals, in which it is difficult to remove the pyrochlore phase, for instance, PZN ($Pb(Zn_{1/3}Nb_{2/3})O_3$), $Pb(Sc_{1/2}Nb_{1/2})O_3$ and PNN($Pb(Nb_{1/3}Nb_{2/3})O_3$) etc.

3.5. XPS analysis of the well-crystallized PMN–PT films

High-resolution XPS is a powerful tool to analyze the chemical states of the elements in the as-developed PMN–PT films and hence helpful to determine the phase purity of the films. The binding energies of the Pb4$f_{7/2}$, Nb3$d_{5/2}$, Ti2$p_{3/2}$ and O1s for the pure-perovskite 0.57PMN–0.43PT films are listed in Table 1, together with the literature data [29], except the data for Mg which is omitted due to low intensity in the spectra.

Table 1
The binding energies (eV) of the Pb, Nb, Ti and O elements in the PMN–PT films.

Samples	Ref.	Pb4$f_{7/2}$		Nb3$d_{5/2}$	Ti2$p_{3/2}$	O1s		
0.57PMN–0.43PT	This work	M	S_{Pb}	M	M	M	S_{O1}	S_{O2}
		138.3	136.1	206.7	458.2	529.7	528.0	532.2
0.63PMN–0.37PT	[29]	M	S_{Pb}			M	S_{O1}	S_{O2}
		138.3	137.1	206.5	457.6	529.4	528.0	532.5
0.53PMN–0.47PT	[29]	M	S_{Pb}			M	S_{O1}	S_{O2}
		138.3		206.9	458.2	529.5	531.2	532.4

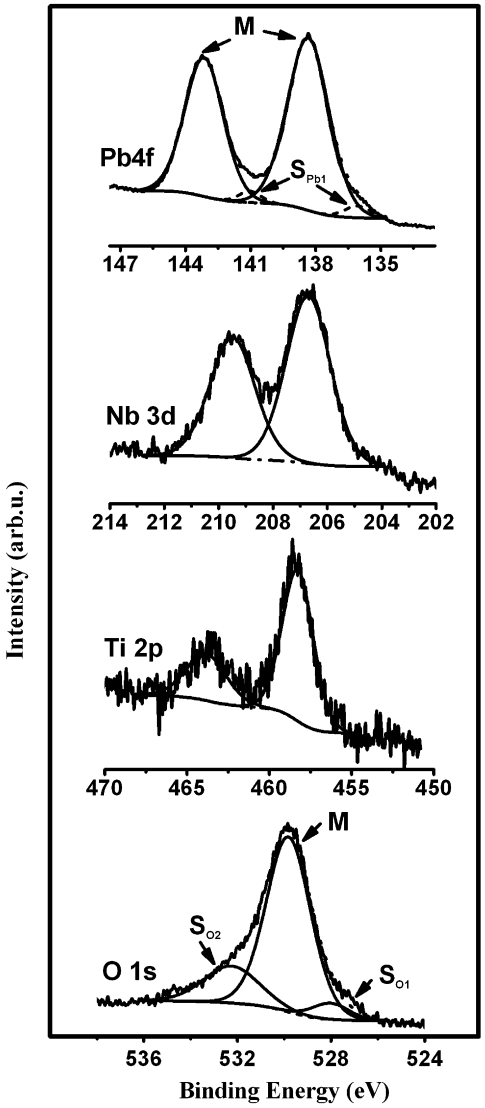

Fig. 5. The high-resolution XPS spectra of the Pb4f, Nb3d, Ti2p and O1s photoelectrons for the 0.57PMN–0.43PT thin films annealed at 650 °C for 30 min.

As shown in Fig. 5, the Pb spectra could be fitted into main (M) and one satellite (S_{Pb}) spin–orbit doublet. The binding energies for the main peaks were 138.3 eV (Pb4$f_{7/2}$) and 143.1 eV (Pb4$f_{5/2}$), and for the satellite peaks were 136.1 eV (Pb4$f_{7/2}$) and 140.9 eV (Pb4$f_{5/2}$). The former could be ascribed to the lattice Pb state, while the latter could belong to metallic state [30], although the reason for the presence of metallic Pb is not clear yet. The Ti2p and Nb3d spectra consisted of only one spin–orbit doublet at Ti2$p_{3/2}$ = 458.2 eV, Ti2$p_{1/2}$ = 463.8 eV and Nb3$d_{5/2}$ = 206.7 eV, Nb3$d_{3/2}$ = 209.5 eV, respectively, which indicated the Ti and Nb ions exhibited only one chemical state. The binding energies for the lattice chemical states of Pb4f, Ti2p and Nb3d are close to those of the 0.63PMN–0.37PT and 0.53PMN–0.47PT single crystals reported in Ref. [29], as shown in Table 1.

The O1s spectra consisted of the main peak and the S_{O1} and S_{O2} satellites with the binding energies of 529.7, 528.0 and 532.2 eV individually. The main peak can be attributed to the lattice oxygen and the S_{O2} results from the surface-absorbed H_2O and CO_2 [31]. The S_{O1} component can be related to structural disorder, as reported in the PMN–PT single crystals with PT content $\leqslant$37% [29]. Structural disorder, the characteristic of relaxor ferroelectrics, suggested random distribution of Nb and Mg ions in the B sites of perovskite lattice and disordered ion displacement [29–32]. Hence the presence of the small SO1 peak indicated our PMN–PT films with 43% PT probably exhibited relaxor behavior.

3.6. Electrical, optical properties of the PMN–PT films

The polarization–electric field (P–E) hysteresis loops of the PMN–PT (43% PT) thin films have been measured under the electric field of 93.5 kV/cm and the results are shown in the inset of Fig. 6. The P–E loop was with the remnant polarization Pr of 7.1 μC/cm and coercive field E_c of 23.5 kV/cm. The dielectric constant of the films as a function of frequency is shown in Fig. 6 and it was decreased with the frequency increasing from 0.1 to 120 kHz. At 1 kHz at room temperature, the dielectric constant and dielectric loss were ~2582 and ~0.10, respectively. The dielectric constants obtained here were comparable to those of the films prepared by pulsed laser deposition [33], and by the other sol–gel processing techniques [27–34].

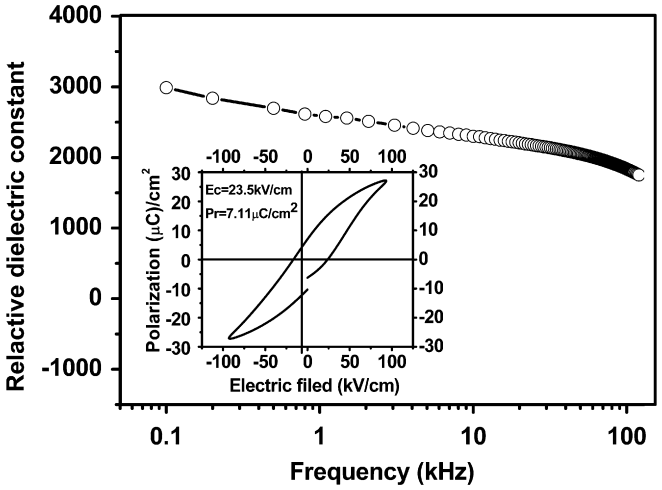

Fig. 6. P–E hysteresis loops (the inset) and dielectric constants vs. frequency (0.1–120 kHz) for the 0.57PMN–0.43PT films.

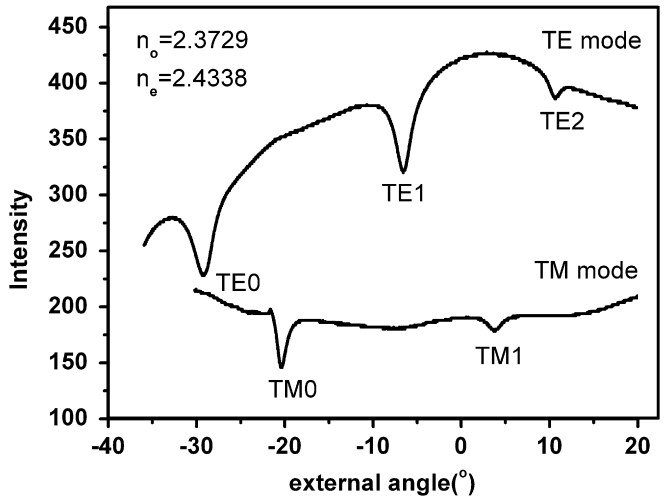

Fig. 7. TE and TM mode spectra for the 0.57PMN–0.43PT thin films at wavelength of 632.3 nm.

Fig. 7 shows the TE (transverse electric, parallel to film surface) and TM (transverse magnetic, perpendicular to the surface) guided-mode spectra for the PMN–PT films. Three TE and two TM modes have been excited for each case. The sharp reflectivity dips indicate a good confinement of light into the waveguide layer of the films. Using all the TE and TM modes in the spectra, the refractive indices of the films can be determined to be $n_{TE} = 2.3729$ and $n_{TM} = 2.4338$, close to 2.5–2.7 for the PMN–PT single crystals and ceramics with PT content above 30% [35]. The transmission measurement shows that the films possessed a high transmittance of 70–80% in the visible wavelength range. These good optical properties can be attributed to the pure-perovskite phase and dense microstructure of the as-developed PMN–PT films.

4. Conclusion

In summary, PMN–PT films with PT% = 23–43% have been synthesized by sol–gel processing with PVP as modifier and lead nitrate as lead source. With PVP addition, perovskite phase directly crystallized from the amorphous films at the temperature as low as 430 °C and the crystallinity was significantly enhanced. Pyrochlore phase can be avoided and pure-perovskite PMN–PT films can be obtained by adding PVP with molecular weight-<630k and at PVP monomer/PMN–PT molar ratio of 0.25–1.0.

XPS analysis indicates that the well crystallized PMN–PT (43% PT) films obtained have the similar lattice chemical states of Pb, Nb, Ti and O ions to those of the counterpart single crystals. The developed films possess the dielectric constant of ~2582 at 1 kHz and the refractive indices of $n_{TE} = 2.3729$ and $n_{TM} = 2.4338$ at $\lambda = 632.3$ nm.

Acknowledgement

The authors would like to acknowledge Defense Advanced Research Projects Agency (DARPA, USA) for their financial support.

Appendix A. Supplementary material

Supplementary data associated with this article can be found in the online version at doi:10.1016/j.jssc.2009.04.021.

References

[1] M.P. Pechini, US Patent no. 3.330.697, 1967.
[2] Q.X. Jia, T.M. Mccleskey, A.K. Burrell, Y. Lin, G.E. Collis, H. Wang, A.D.Q. Li, S.R. Foltyn, Nat. Mater. 3 (2004) 529.
[3] M.A. Gülgün, M.H. Nguyen, W.M. Kriven, J. Am. Ceram. Soc. 82 (1999) 556.
[4] S.J. Lee, E.A. Benson, W.M. Kriven, J. Am. Ceram. 82 (1999) 2049.
[5] P. Lin, W. Ren, X.Q. Wu, P. Shi, X. Yan, X. Yao, J. Appl. Phys. 102 (2007) 0841091.
[6] K. Yao, S. Yu, F.E.H. Tay, Appl. Phys. Lett. 88 (2006) 052904–052913.
[7] S. Yu, K. Yao, F.E.H. Tay, Chem. Mater. 18 (2006) 5343–5350.
[8] H. Kozuka, S. Takenaka, H. Tokita, M. Okubayashi, J. Europ. Ceram. Soc. 24 (2007) 1585.
[9] S. Takenaka, H. Kozuka, Appl. Phys. Lett. 79 (2001) 3485.
[10] Z.H. Du, J. Ma, T.S. Zhang, J. Am. Ceram. Soc. 90 (2007) 815.
[11] S. Linardos, Q. Zhang, J.R. Alcock, J. Europ. Ceram. Soc. 26 (2006) 117.
[12] M. Liao, X.L. Zhong, J.B. Wang, H.L. Yan, J.P. He, Y. Qiao, Y.C. Zhou, J. Cryst. Growth 304 (2007) 69.
[13] Z.H. Du, T.S. Zhang, J. Ma, J. Mater. Res. 22 (2007) 2195–2203.
[14] W. Gong, J.F. Li, X. Chu, L. Li, J. Am. Ceram. Soc. 87 (2004) 1031–1034.
[15] H. Beltrán, E. Cordoncillo, P. Escribano, J.B. Carda, A. Coats, R. Anthony, West Chem. Mater. 12 (2000) 400–405.
[16] N. Wakiya, J. Shiihara, K. Shinozaki, N. Mizutanil, J. Solid Stat.Chem. 142 (1999) 344–348.
[17] S. Parola, R. Khem, D. Cornu, J. Sol–Gel Sci. Technol. 26 (2003) 1109–1112.
[18] J.H. Park, D.H. Kang, K.H. Yoon, J. Am. Ceram. Soc. 82 (1999) 2116–2120.
[19] Z. Zhang, B. Zhao, L. Hu, J. Solid Stat. Chem. 121 (1996) 105–110.
[20] M. Liu, X. Yan, H. Liu, W. Yu, React. Funct. Polymers 44 (2000) 55–64.
[21] T. Saegusa, Pure Appl.Chem. 67 (1995) 1965.
[22] Z.H. Du, T.S. Zhang, M.M. Zhu, J. Ma, J. Mater. Res. 24 (2009) 1576–1584.
[23] Z.H. Du, T.S. Zhang, M.M. Zhu, J. Ma, J. Appl. Phys. 105 (2009), doi:10.1063/1.3056165.
[24] H. Beltrán, E. Cordoncillo, P. Escribano, J.B. Carda, A. Coats, A.R. West, Chem. Mater. 12 (2000) 400–405.
[25] C. Boudaren, J.P. Auffrédic, P.B.B. Rocherullé, D. Louër, Sol. Stat. Sci. 3 (2001) 847–858.
[26] S.M.K. Nair, K.K. Malayil, Thermochim. Acta 129 (1988) 237–247.
[27] T.C. Goel, P. Kumar, A.R. JAMES, C. Prakash, J. Electroceram. 13 (2004) 503–507.
[28] J.H. Park, F. Xu, S. Trolier-McKinstry, J. Appl. Phys. 89 (2001) 568–574.
[29] A. Kania, E. Talik, M. Kruczek, A. Słodczyk, J. Phys. Condens. Matter 17 (2005) 6737–6749.
[30] C.D. Wagner, W.M. Riggs, L.E. Davis, J.F. Moulder, Handbook of X-Ray Photoelectron Spectroscopy, Perkin–Elmer Corporation Physical Electronics, Eden Prairie, 1979, p. 160.
[31] S. Takatani, H. Miki, K. Kushida-Abdelghafar, K. Torii, J. Appl. Phys. 85 (1999) 7784.
[32] L.E. Cross, Ferroelectrics 76 (1987) 241–267.
[33] Y. Wang, Y.L. Cheng, K.C. Cheng, H.L.W. Chan, C.L. Choy, Appl. Phys. Lett. 85 (2004) 1580–1582.
[34] J.H. Park, D.H. Kang, K.H. Yoon, J. Am. Ceram. Soc. 82 (1999) 2116–2120.
[35] X. Wan, H.L.W. Chan, C.L. Choy, X. Zhao, H. Luo, J. Appl. Phys. 96 (2004) 1387–1391.